

Thermal analysis of an SOA integrated in SG-DBR laser module

Ximeng Han¹ · Jinwei Gao¹ · Hao Wang¹ · Yonglin Yu¹

Received: 29 September 2015 / Accepted: 19 January 2016 / Published online: 27 January 2016
© Springer Science+Business Media New York 2016

Abstract In this paper, we developed a temperature-dependent thermal-optical model of a semiconductor optical amplifier (SOA) integrated in sampled grating distributed Bragg reflector (SG-DBR) laser module by extending our previous works. By numerically solving the thermo-optical coupling equations, static and transient temperature distributions of the integrated module were simulated based on finite element method (FEM). Furthermore, thermal effects on optical output properties of the module were obtained by using a temperature-dependent dynamic transfer matrix method (DTMM) based optical model. Phenomenon of thermal crosstalk was clearly observed. Induced by the thermal transients in the SOA, the wavelength drift is as large as 39 pm and the power decrease is over 5 %. Our results could be helpful to the design optimization and the thermal management of relevant integrated devices.

Keywords SOA · SG-DBR laser · FEM · DTMM · Thermal wavelength drift

1 Introduction

With the rapid development of optical fiber communication technology, SG-DBR laser as a typical monolithically integrated tunable laser transmitter has become one of the core components in novel dynamic wavelength division multiplexing (DWDM) optical

This article is part of the Topical Collection on Numerical Simulation of Optoelectronic Devices, NUSOD' 15.

Guest edited by Julien Javaloyes, Weida Hu, Slawek Sujecki and Yuh-Renn Wu.

✉ Yonglin Yu
yonglinyu@mail.hust.edu.cn

¹ Wuhan National Laboratory for Optoelectronics, Huazhong University of Science and Technology, Wuhan 430074, People's Republic of China

networks (Coldren 2014). SG-DBR laser offers compelling merits in terms of small volume, low power dissipation, wide wavelength tuning range, fast wavelength switching, flexible output wavelengths, etc. (Coldren et al. 2011). Thus timely and effective inventory management and channel fast-building function could be provided, the cost of alternative schemes of light source would be greatly reduced. Technologies in the next generation reconfigurable optical networks such as wavelength automatic configuration, wavelength conversion and wavelength routing may also benefit a lot. (Yu and O'Dowd 2001; Buis and Murphy 2006; Browning et al. 2013). For device diversification in photonic integrated circuits (PICs), SG-DBR lasers are usually integrated with many active and passive devices functionally, for instance, an SOA is typically integrated with an SG-DBR laser to amplify, equalize and modulate the output power (Nicholes et al. 2010; Shu et al. 2012; Yu et al. 2014). In recent years, the performance degradation problems of the photonic integrated devices induced by thermal effects gradually attract investigators' eyes (Puttnam et al. 2005; Kozodoy et al. 2005; Connolly et al. 2006). Puttnam et al. (2005) confirmed that thermal effects caused by current switching gave rise to output wavelength drift when they used an SG-DBR laser to conduct transmission experiments in WDM system. The drift would lead to crosstalk in channels and result in increased bit error rate during the transmission. Using an SOA and an electro-absorption modulator (EAM) integrated with an SG-DBR laser, Kozodoy et al. (2005) carried out test experiments and found thermal crosstalk in each integrated device would affect device performance unfavorably. In our previous work, we have elaborately approved theoretical analysis and simulated the thermal transients in SG-DBR lasers (Wang and Yu 2012). A theoretical model capable of calculating temperature distribution and simulating the dynamic lasing behavior of an SG-DBR tunable laser with the influence of thermal effects into account was proposed. By extending our previous works in this paper, we proposed a temperature-dependent thermo-optical model of an SOA integrated in SG-DBR laser module. By numerically solving the thermo-optical coupling equations, the static and transient 3D temperature distributions of the integrated module are obtained based on FEM. Thermal effects on device performance (optical output properties) are discussed by using the temperature-dependent DTMM based optical model. Phenomenon of thermal crosstalk is clearly observed.

2 Physical and mathematical model of an SOA integrated in SG-DBR laser module

To amplify, equalize and modulate the output signal power, an SOA is usually integrated at the output end of SG-DBR laser as illustrated in Fig. 1a. Passing the active region of SOA, output power of the light will be boosted related to stimulated emission.

Temperature $T(x, y, z, t)$, photon density $S(z)$ and carrier density $N(z)$ distributions in the SOA are related to each other. We proposed the thermal model of an SOA contains

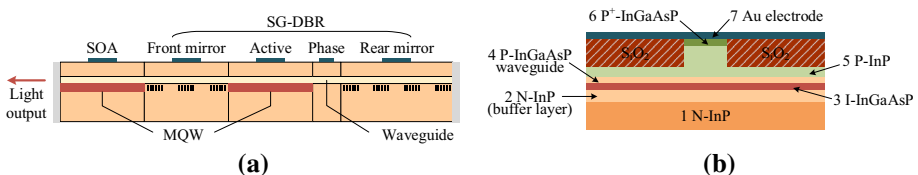


Fig. 1 **a** Schematic diagram of the tunable SG-DBR laser integrated with SOA, **b** cross section of the SOA

thermo-optical coupling equations consist of heat conduction equation, carrier density equation and photon density equation that can be worked out $T(x, y, z, t)$, $S(z)$ and $N(z)$ base on FEM. Corresponding equations are as follows:

- Heat conduction equation

$$\frac{\partial T(x, y, z, t)}{\partial t} - \frac{K}{\rho C} \nabla^2 T(x, y, z, t) = \frac{Q(x, y, z, t)}{\rho C} \tag{1}$$

where (x, y, z) is the space coordinates, t is the time, K is the thermal conductivity, ρ is the density, C is the specific heat and $Q(x, y, z, t)$ is the heat generation rate defined as heat generation power in unit volume.

- Photon density equation

$$\frac{dS(z)}{dz} = \Gamma g_{net}(z)S(z) \tag{2}$$

where Γ is the optical confinement factor, g_{net} is the net gain;

- Carrier density equation

$$\frac{j}{ed} = g(z)v_g S(z) + R(z) \tag{3}$$

where j is the injection current density, e is the electron charge, d is the thickness of active region, g is the gain, v_g is the group velocity and R is the carrier recombination rate which can be expressed as:

$$R(z) = Ae^{\frac{E_1}{k_B} \left(\frac{1}{T_0} - \frac{1}{T} \right)} N(z) + Be^{\frac{E_2}{k_B} \left(\frac{1}{T_0} - \frac{1}{T} \right)} N(z)^2 + Ce^{\frac{E_3}{k_B} \left(\frac{1}{T_0} - \frac{1}{T} \right)} N(z)^3 \tag{4}$$

Simplified as:

$$R(z) = e^{3.9(1-T_0/T)} [AN(z) + BN(z)^2 + CN(z)^3] \tag{5}$$

where A , B and C are the non-radiative recombination coefficient, bimolecular recombination coefficient and auger recombination coefficient under temperature T_0 (300 K), E_1 , E_2 and E_3 are the activation energy according to the recombination respectively (about 0.1 eV) and k_B is the Boltzmann constant. Substituting (5) into (3), we rearrange and then get new equation

$$\frac{j}{ed} = g(z)v_g S(z) + e^{3.9(1-T_0/T)} [AN(z) + BN(z)^2 + CN(z)^3] \tag{6}$$

besides, g and g_{net} in Eqs. (2) and (3) can be expressed as follows:

$$g = g_N \frac{T_0}{T} \left(N - N_0 \frac{T}{T_0} \right) / \left[1 + g_{cf} \cdot S(z) \right] \tag{7}$$

$$g_{net} = g - \left(\frac{a_0}{\Gamma} + a_N N \right) \tag{8}$$

where g_N is the differential gain, a_N is the differential loss, N_0 is the carrier density at transparency, g_{cf} is the gain compression factor, a_0 is the optical loss without carrier injection.

Structure and working principle of the SOA and the active section of SG-DBR laser are extremely similar, so heat generation rates Q_i ($i = 1-7$) in Eq. (1) of each layer in SOA are

similar to those of the SG-DBR laser's (Wang and Yu 2012). Figure 1b shows the cross section of SOA, numbers 1–7 in the figure refer to different epitaxial layers with different heat generation rates (Kobayashi and Furukawa 1975). In particular, for the heat generation rate Q_3 of I-InGaAsP active layer, we should take the longitudinal nonuniformity of carrier density and photon density into account. Then Q_3 can be expressed as:

$$Q_3(z) = \frac{V_j(1 - \eta_{sp}f_{sp})}{d} \cdot [edR(z) + (j - edR(z))(1 - \eta_i)] \quad (9)$$

where V_j is the junction voltage, η_{sp} and η_i are the internal quantum efficiencies of spontaneous emission and stimulated emission respectively, f_{sp} is the ratio of escaped spontaneous emission photons from active region to all the spontaneous emission photons. In these cases, we solve the coupling Eqs. (1)–(3) based on FEM and then analyze certain static and transient problems of the SOA. Furthermore, we established an extended and more comprehensive thermo-optical model of SG-DBR laser integrated with SOA by coupling thermo-optical model of the SOA and thermo-optical model of the SG-DBR laser (Wang and Yu 2012). Accordingly, we could calculate static and transient temperature, carrier density and photon density distributions of the whole module then. It should be noticed that our thermal model is 3D while our optical model is 1D (in z -axis direction). When we coupled these two models, 1D temperature distribution extracted from 3D temperature distribution results was used. So there are some approximate errors, however, they can be ignored in practice.

3 Simulation and analysis

Parameters (e.g. geometry, material and injection current of each section of the module), initial conditions and boundary conditions were given as follow. Length of the SOA is 300 μm . I_{SOA} is injection current of the SOA, I_f , I_a , I_p and I_r are injection currents of the four sections of SG-DBR laser respectively, T_a is the ambient temperature (300 K), P_0 is the optical input power of the SOA. Lower surface of the AlN submount contacts with a heat sink, consequently we set it as a constant temperature boundary (300 K). The other surfaces are all set as heat convection boundary where their heat convection coefficient h is 20 $\text{W m}^{-2} \text{K}^{-1}$. The other parameters in our simulation are the same as those in reference (Wang and Yu 2012).

In these cases, by using our model and software COMSOL based on FEM, static temperature distribution of the module was worked out firstly. In Fig. 2, (a) shows the geometric model of the module and the initial static temperature distribution without injection currents; (b) manifests the static temperature distribution when $I_{SOA} = I_f = I_p = 0$, $I_a = 100 \text{ mA}$, $I_r = 45 \text{ mA}$ and $P_0 = 5.2 \text{ mW}$; (c) manifests the static temperature distribution when $I_{SOA} = 180 \text{ mA}$, $I_f = I_p = 0$, $I_a = 100 \text{ mA}$, $I_r = 45 \text{ mA}$ and $P_0 = 5.2 \text{ mW}$; (d) manifests the 1-D longitudinal static temperature distribution across the center of the laser's active region. As shown in Fig. 2b, c, we observed that temperature in the SOA is much higher than those of other sections in this module when I_{SOA} switches to 180 mA. As shown in Fig. 2d, thermal crosstalk between SOA and front mirror section is observed: there is about a 3 K temperature rise in the front mirror section induced by temperature rise in the SOA which may lead to unacceptable wavelength drift.

Not only for power amplification and equilibrium, but also the integrated SOA can be used as a "photo switch" with a function of output masking during the wavelength

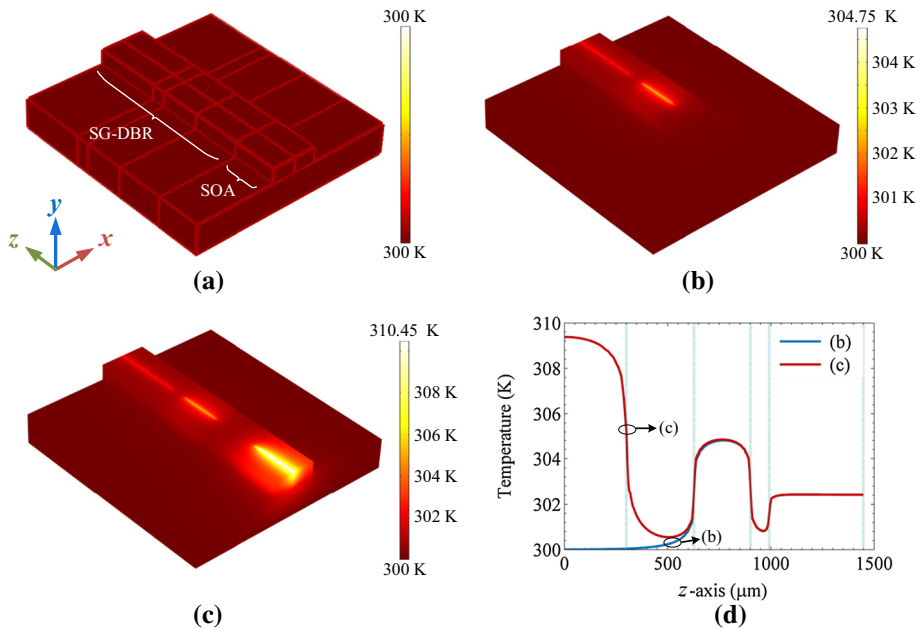
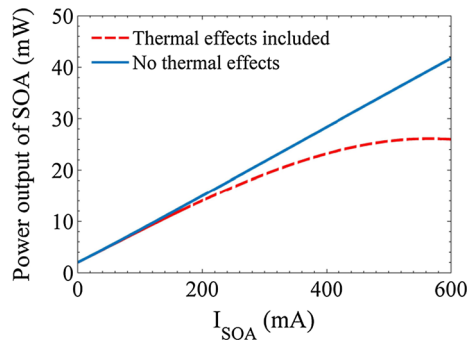


Fig. 2 **a** Geometric model of the module in COMSOL and initial static temperature distribution without injection currents, **b** static temperature distribution when $I_{SOA} = I_f = I_p = 0$, $I_a = 100$ mA, $I_r = 45$ mA and $P_0 = 5.2$ mW, **c** static temperature distribution when $I_{SOA} = 180$ mA, $I_f = I_p = 0$, $I_a = 100$ mA, $I_r = 45$ mA and $P_0 = 5.2$ mW, **d** longitudinal static temperature distribution across the center of the laser’s active region under situations **b** and **c**

Fig. 3 Optical output power of SOA with/without taking thermal effect into account, when I_{SOA} is set from 0 to 600 mA and P_0 remains 5.2 mW



switching process to keep away the laser transmitter from adverse impacts caused by transient changes. When the injection current of the SOA switches, its output power “switches” accordingly. The changes of injection current may lead to carrier density changes, and further give rise to a dynamic temperature variation which would influence the band gap, refraction and many other physical parameters (Camassel et al. 1975; Smith et al. 1997). By using a temperature-dependent DTMM based optical model (Wang and Yu 2012), we obtained thermally induced wavelength drift and optical output power of the module.

Figure 3 manifests optical output power of the SOA with taking thermal effect into account or not, when I_{SOA} are set from 0 to 600 mA, $I_f = I_p = 0$, $I_a = 100$ mA,

$I_r = 45$ mA and $P_0 = 5.2$ mW. Optical output power of the SOA P_{out} is closely related to the temperature: when I_{SOA} is small at the beginning, P_{out} increases with I_{SOA} increasing (0–200 mA); if I_{SOA} continues to increase (200–600 mA), P_{out} will almost-linearly increase without taking thermal effects into account as the blue curve shown, while the thermal effects caused by injection current of SOA would give rise to a saturated optical output power $P_{out,S}$ as the red curve shown. Evidently, output power of the module is influenced by the thermal effects.

Then, we calculated transient temperature distributions of the SOA (red curves) and the front mirror section (blue curves) with $I_f = I_p = 0$, $I_a = 100$ mA, $I_r = 45$ mA, $P_0 = 5.2$ mW when SOA switches on (I_{SOA} switches from 0 to 110 and 180 mA respectively) as illustrated in Fig. 4. According to the temperature rise in front mirror section within 10^{-6} s time delay, the transient temperature variation in front mirror section is seen mainly caused by thermal crosstalk from the SOA.

Figure 5 gives the impact of thermal transient on the device performance including thermal induced wavelength drifts and output power variations under the same conditions as described in Fig. 4. Thermal induced wavelength drift is as large as 39 pm and power output approximately falls from 13.66 to 12.93 mW (falls nearly 5.3 %) in the time order of 10^{-3} s when I_{SOA} switches from 0 to 180 mA. When I_{SOA} switches from 0 to 110 mA, corresponding wavelength drift is about 20 pm and power output approximately falls from 9.04 to 8.78 mW (falls nearly 2.9 %) in the same time scale. For the optical burst switching (OBS) application in dynamic optical networks, the integrated SOA is used as an optical switch to fulfill “output blanking” function during wavelength switching, where the SOA is needed to switch off and switch on in about 500 ns, and keep on the “switch on” state in

Fig. 4 Transient temperature distributions of the SOA and the front mirror section with $I_f = I_p = 0$, $I_a = 100$ mA, $I_r = 45$ mA, $P_0 = 5.2$ mW, when SOA switches on

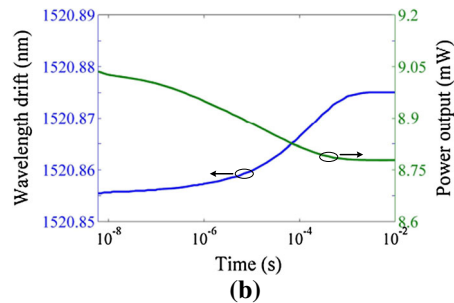
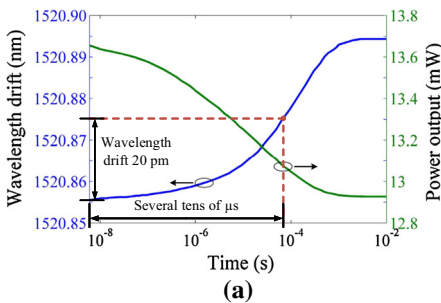
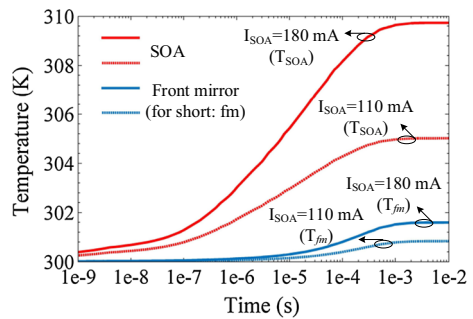


Fig. 5 Thermal wavelength drift and power output variations when SOA switches on. **a** I_{SOA} from 0 to 180 mA, **b** I_{SOA} from 0 to 110 mA

one burst period (a few hundred μs or even several ms). According to ITU-T standard, the minimum tolerance of wavelength deviation to the center wavelength of each channel is ± 20 nm (frequency deviation ± 2.5 GHz) in a typical 50 GHz DWDM system. As the simulated results shown in Fig. 5a in our paper, the wavelength drift induced by thermal effects of the integrated SOA can reach 20 nm in about 100 μs which will cause unacceptable thermal crosstalk between the channels. If I_{SOA} is set larger than 200 mA (Webb et al. 2011), the thermal transients will be more obvious.

4 Conclusion

A temperature-dependent thermo-optical model of an SOA integrated in SG-DBR laser module is developed based on our previous works. By numerically solving thermo-optical coupling equations of the model, static and transient temperature distributions of the integrated module are simulated based on FEM. Thermal crosstalk between the SOA and the front mirror section of SG-DBR laser are observed. Besides, thermal transient in the front mirror section is mainly caused by the thermal crosstalk from the SOA in switching processes of it within a 10^{-6} s time delay. By using a temperature-dependent DTMM based optical model, thermally induced wavelength drift and optical output power are discussed. Taking thermal effects into account in our simulation, the results indicate that thermal effects may affect optical output properties of the module evidently. Wavelength drift induced by thermal transients in the SOA is as large as 39 nm and output power decrease is about 5.3 % when I_{SOA} switches from 0 to 180 mA. If I_{SOA} is set larger, the thermal transients will be much more obvious. Our results could be helpful to the design optimization and the thermal management of such integrated devices.

Acknowledgments The authors acknowledge the supports provided by the National Natural Science Foundation of China under Grant 11,174,097, the National High Technology Developing Program of China under Grant No. 2013AA014503, and the International S&T Cooperation Program of China (1016).

References

- Browning, C., Shi, K., Ellis, A.D., Barry, L.P.: Optical burst-switched SSB-OFDM using a fast switching SG-DBR laser. *J. Opt. Commun. Netw.* **5**, 994–1000 (2013)
- Buus, J., Murphy, E.J.: Tunable lasers in optical networks. *J. Lightwave Technol.* **24**, 5–11 (2006)
- Camassel, J., Auvergne, D., Mathieu, H.: Temperature dependence of the band gap and comparison with the threshold frequency of pure GaAs lasers. *J. Appl. Phys.* **46**, 2683–2689 (1975)
- Coldren, L. A. In: IEEE International Semiconductor Laser Conference, pp. 48–49 (2014)
- Coldren, L.A., Nicholes, S.C., Ristic, S., Guzzon, R.S., Norberg, E.J., Krishnamachari, U.: High performance InP-based photonic ICs. *J. Lightwave Technol.* **29**, 554–570 (2011)
- Connolly, E., Kaszubowska-Anandarajah, A., Barry, L. P. In: IEEE International Conference on Transparent Optical Networks, pp. 52–55 (2006)
- Kobayashi, T., Furukawa, Y.: Temperature distributions in the GaAs-AlGaAs double-heterostructure laser below and above the threshold current. *Jpn. J. Appl. Phys.* **14**, 1981–1986 (1975)
- Kozodoy, P., Strand, T.A., Akulova, Y.A.: Thermal effects in monolithically integrated tunable laser transmitters. *IEEE Trans. Compon. Packag. Technol.* **28**, 651–657 (2005)
- Nicholes, S.C., Mašanović, M.L., Jevremović, B., Lively, E., Coldren, L., Blumenthal, D.J.: An 8 × 8 InP monolithic tunable optical router (MOTOR) packet forwarding chip. *J. Lightwave Technol.* **28**, 641–650 (2010)
- Puttnam, B., Dueser, M., Bayvel, P. In: Optical Fiber Communication Conference, pp. JWA30 (2005)
- Smith, W.R., King, J.R., Tuck, B.: Mathematical modelling of thermal effects in semiconductor laser operation. *IEE J. Proc. Optoelectron.* **144**, 389–396 (1997)

- Shu, T., Yu, Y.L., Lv, H., Huang, D.X., Shi, K., Barry, L.: Influence of facet reflection of SOA on SOA-integrated SGDBR laser. *Front. Optoelectron.* **5**, 390–394 (2012)
- Wang, H., Yu, Y.L.: New theoretical model to analyze temperature distribution and influence of thermal transients of an SG-DBR laser. *IEEE J. Quantum Electron.* **48**, 107–113 (2012)
- Webb, R.P., Dailey, J.M., Manning, R.J., Ellis, A.D.: Phase discrimination and simultaneous frequency conversion of the orthogonal components of an optical signal by four-wave mixing in an SOA. *Opt. Express* **19**, 20015–20022 (2011)
- Yu, L., Lu, D., Pan, B., Zhao, L.: Widely tunable optical decision circuit using a monolithically integrated SOA-SGDBR laser. *IEEE Photonic Technol. Lett.* **26**, 722–725 (2014)
- Yu, Y., O'Dowd, R.: Fast intra-modal and inter-modal wavelength switching of a high-speed SG-DBR laser for dynamic wavelength routing. *Opt. Quantum Electron.* **33**, 641–652 (2001)